Title

Reliance of Wolbachia on High Rates of Host Proteolysis Revealed by a Genome-Wide RNAi Screen of Drosophila Cells

Journal

Genetics, 205(4)

ISSN

0016-6731

Authors

White, Pamela M
Serbus, Laura R
Debec, Alain
et al.

Publication Date

2017-04-01

DOI

10.1534/genetics.116.198903

Peer reviewed

Reliance of *Wolbachia* on High Rates of Host Proteolysis Revealed by a Genome-Wide RNAi Screen of *Drosophila* Cells

Pamela M. White,*[,1] Laura R. Serbus,[†,‡,1] Alain Debec,[§] Adan Codina,* Walter Bray, Antoine Guichet,[§] R. Scott Lokey,** and William Sullivan*[,2]**

*Department of Molecular, Cell, and Developmental Biology and **Department of Chemistry and Biochemistry, University of California, Santa Cruz, California 95064, [†]Department of Biological Sciences and [‡]Biomolecular Sciences Institute, Florida International University, Miami, Florida 33199, and [§]Institut Jacques Monod, Centre National de la Recherche Scientifique, Unité Mixte de Recherche 7592, University Paris Diderot, 75 205 Paris, France

ABSTRACT *Wolbachia* are gram-negative, obligate, intracellular bacteria carried by a majority of insect species worldwide. Here we use a *Wolbachia*-infected *Drosophila* cell line and genome-wide RNA interference (RNAi) screening to identify host factors that influence *Wolbachia* titer. By screening an RNAi library targeting 15,699 transcribed host genes, we identified 36 candidate genes that dramatically reduced *Wolbachia* titer and 41 that increased *Wolbachia* titer. Host gene knockdowns that reduced *Wolbachia* titer spanned a broad array of biological pathways including genes that influenced mitochondrial function and lipid metabolism. In addition, knockdown of seven genes in the host ubiquitin and proteolysis pathways significantly reduced *Wolbachia* titer. To test the *in vivo* relevance of these results, we found that drug and mutant inhibition of proteolysis reduced levels of *Wolbachia* in the *Drosophila* oocyte. The presence of *Wolbachia* in either cell lines or oocytes dramatically alters the distribution and abundance of ubiquitinated proteins. Functional studies revealed that maintenance of *Wolbachia* titer relies on an intact host Endoplasmic Reticulum (ER)-associated protein degradation pathway (ERAD). Accordingly, electron microscopy studies demonstrated that *Wolbachia* is intimately associated with the host ER and dramatically alters the morphology of this organelle. Given *Wolbachia* lack essential amino acid biosynthetic pathways, the reliance of *Wolbachia* on high rates of host proteolysis via ubiquitination and the ERAD pathways may be a key mechanism for provisioning *Wolbachia* with amino acids. In addition, the reliance of *Wolbachia* on the ERAD pathway and disruption of ER morphology suggests a previously unsuspected mechanism for *Wolbachia's* potent ability to prevent RNA virus replication.

KEYWORDS *Wolbachia*; RNAi; *Drosophila*; oocyte; ubiquitin; virus

WOLBACHIA is a bacterial endosymbiont present in insects and filarial nematodes (Serbus *et al.* 2008; Werren *et al.* 2008). *Wolbachia* resides in both somatic and germline cells of its male and female insect hosts (Pietri *et al.* 2016). The evolutionary success of *Wolbachia* depends on efficient vertical transmission through the female germline. This is facilitated by *Wolbachia* localization to the posterior pole of the oocyte, ensuring its incorporation into the germline of the next generation. To achieve this, *Wolbachia* rely on host microtubules, motor proteins, and an interaction with the host pole plasm components (Kose and Karr 1995; Ferree *et al.* 2005; Serbus and Sullivan 2007). The success of *Wolbachia* also requires regulation of bacterial abundance within host somatic and germline cells. Underreplication of *Wolbachia* in the oocyte results in inefficient vertical transmission and overreplication of *Wolbachia* results in disruption of critical host cellular functions (Serbus *et al.* 2011; Newton *et al.* 2015). Cytological and PCR-based studies demonstrate that recently caught wild strains of *Drosophila* exhibit tremendous variability in *Wolbachia* titer (Unckless *et al.* 2009). These variations not only occur from one individual to another

doi: https://doi.org/10.1534/genetics.116.198903
Manuscript received December 1, 2016; accepted for publication January 27, 2017; published Early Online February 2, 2017.
Supplemental material is available online at www.genetics.org/lookup/suppl/doi:10.1534/genetics.116.198903/-/DC1.
[1]These authors contributed equally to this work.
[2]Corresponding author: Department of Molecular, Cell, and Developmental Biology, University of California, Santa Cruz, 1156 High St., Santa Cruz, CA 95064. E-mail: wtsulliv@ucsc.edu

but also between tissues within an individual (Albertson *et al.* 2009; Muller *et al.* 2013).

A combination of host and *Wolbachia* factors as well as the environment influence *Wolbachia* abundance. For example, in the *Drosophila* oocyte, *Wolbachia* rely on normal host microtubule organization and the Gurken dorsal signaling complex to maintain titer (Ferree *et al.* 2005; Serbus *et al.* 2011). Additional evidence for the influence of host factors on *Wolbachia* titer comes from the finding that the same *Wolbachia* strain in *D. simulans* and *D. melanogaster* exhibits dramatically different titers in the mature oocyte (Poinsot *et al.* 1998; Serbus and Sullivan 2007). Evidence that factors intrinsic to *Wolbachia* influence its titer comes from the identification of the *Wolbachia* variant, *w*MelPop. The *w*MelPop strain exhibits extremely high titers in the central nervous system relative to other *Wolbachia* strains, independent of the host strain or species in which it resides (Min and Benzer 1997). Finally, extrinsic environmental factors such as temperature and diet dramatically influence *Wolbachia* titer (Mouton *et al.* 2006; Serbus *et al.* 2015). These changes are moderated in part through the host insulin signaling pathway (Serbus *et al.* 2015)

To comprehensively identify host factors that influence *Wolbachia* titer, we have employed a genome-wide RNA interference (RNAi) screen using a *Drosophila* cell line infected with *Wolbachia*. Our approach was motivated by the success of a number of previous cell-based screens using *Drosophila* cell lines (Mohr *et al.* 2014). Using *Drosophila* cells, genome-wide RNAi screens were performed to identify host genes that alter *Listeria monocytogenes*, *Mycobacterium fortuitum*, *Chlamydia caviae*, and *Francisella tularensis* infection and proliferation (Agaisse *et al.* 2005; Philips *et al.* 2005; Derre *et al.* 2007; Akimana 2010). We specifically assayed for RNAi-mediated gene knockdowns that either up- or down-regulate *Wolbachia* titer. The cell line was created from primary embryonic cultures of *Drosophila melanogaster* infected with *w*Mel *Wolbachia* strain (Serbus *et al.* 2012). *Wolbachia* is stably maintained in these cultures and exhibits a close association with microtubules as found in *Drosophila* somatic and germline tissues (Kose and Karr 1995; Albertson *et al.* 2009). The cell line expresses a transgene encoding the GFP-tagged gene *Jupiter*, which encodes a microtubule-associated protein that labels microtubules and facilitates high-throughput, cell-based screening approaches (Karpova *et al.* 2006). The *Wolbachia*-infected cells were originally employed for high-throughput, cell-based screens to identify small molecule inhibitors of *Wolbachia* (Serbus *et al.* 2012; Van Voorhis *et al.* 2016). By combining genome-wide RNAi approaches with automated microscopy, we were able to screen the majority of the *Drosophila* genome for those genes that influence *Wolbachia* titer. As described below, this analysis yielded a number of host genes critical for regulating intracellular *Wolbachia* titer and revealed that the host ubiquitin and proteolysis pathways play an especially critical role in maintaining *Wolbachia* titer.

Materials and Methods

Generation of cultured cells

The JW18 cell line bearing the Jupiter-GFP transgene was generated according to previously described methods (Karpova *et al.* 2006; Serbus *et al.* 2012; Debec *et al.* 2016). Two- to 15-hour-old embryos derived from *Wolbachia*-infected flies carrying a Jupiter-GFP transgene were homogenized and plated in flasks. During the next 6 months of maintenance, 5 of the initial 20 seed flasks converted into immortal tissue culture lines. The JW18 cell line was selected for further pursuit due to its planar growth pattern and stably abundant *Wolbachia* infection. Cells were maintained at 25–26° in Sang and Shields media containing 10% fetal bovine serum, split weekly at a 1:2 dilution. A cured version of the JW18 line, referred to as JW18DOX, was generated by treating the cells with doxycycline. Electron microscopy was primarily performed on a second *Wolbachia*-infected cell line that expressess Jupiter-GFP and Histone-RFP (LDW1) generated as described above.

Screening approach

Two different *Drosophila* RNAi libraries were used in this screen: UCSF DmRNAi library version 1 and UCSF DmRNAi library version 2. These libraries have been used previously in Echard *et al.* (2004) and Goshima *et al.* (2007). Both libraries are available in 96-well format from Open Biosystems, now a part of GE Healthcare. Three out of four wells from each 384-well screening plate (Griener Bio-one) were set aside for experimental use. The fourth quadrant of wells was used for controls to define baselines for (1) untreated wells with standard levels of infected cells and (2) wells carrying significant reductions in infection, as induced by pararosaniline pamoate, administered to 100 μM final concentration (Serbus *et al.* 2012). JW18 cells without serum were added at a concentration of 6500 cells per well to a plate precoated with 0.5 mg/ml Concanavalin A. After the cells adhered to the plates for 50 min, double-stranded RNA (dsRNA) was transferred into the plate of JW18 cells using a Janus MDT pin tool and media containing 40% fetal bovine serum (FBS) was added for a final concentration of 10% FBS. The average concentration of dsRNA was 0.223 μg/well. All treatments were distributed into two plate replicates. After a 5-day incubation with the dsRNAs at 25°, the cells were prepared for imaging. Cells were fixed for 20 min in 4% formaldehyde and rinsed with PBS using an automated BioTek liquid handler. All staining solutions were administered using a Multidrop robot, with extensive rinsing between treatments. Mouse anti-histone (MAB052, Millipore, Bedford, MA) and goat anti-mouse Alexa 594 (Invitrogen, Carlsbad, CA) was diluted to 1:1250 in PBS/0.1% Triton. A stock solution saturated with DAPI was used at a final concentration of 1:40. After staining, PBS+sodium azide was added to all wells of the plates.

Screen data analysis

Stained plates were imaged using an ImageXpress Micro system (Molecular Devices, Sunnyvale, CA). Ten images were

acquired per well at ×40 magnification. These images were analyzed using customized analysis software provided by Molecular Devices. The software routine masks any areas where clumps of cells are detected, then detects boundaries of the cells and nuclei based upon Jupiter-GFP and anti-histone stains. A mask was applied to the nuclei to obscure fluorescent signal from those areas. Thresholds for DAPI fluorescence detection were set to maximize *Wolbachia* detection while minimizing the background DAPI signal in pararosaniline pamoate-treated control cells, then applied to analysis of the entire plate. Cytoplasmic DAPI attributable to *Wolbachia* nucleoids was scored in each cell to classify it as *Wolbachia*-infected or uninfected. A spreadsheet from the data analysis software indicated the quantity of *Wolbachia*-infected cells *vs.* total cells measured in each well. Average and standard deviation values were calculated for the frequency of Wolbachia infection in JW18 and pararosaniline pamoate-treated JW18 control cells, using the descriptive statistics function in Statistical Package for the Social Sciences (SPSS by IBM). These values were used to calculate a Z′ factor for each plate. The Z′ factor represents one – (three multiplied by the absolute value of the sum of the SD for each control divided by the absolute value of the difference between mean values for each control) (Zhang *et al.* 1999). Z′ factors regarded as acceptable in this field range from 0 to 1. Our Z′ factors ranged from 0.25 to 0.85 per plate, confirming that the controls were clearly distinguishable by the assay. To identify preliminary "hit" compounds that substantially reduced intracellular *Wolbachia* titer, an initial hit range was calculated to lie between the JW18 average infection frequency − 3 SD, and the average pararosaniline pamoate-treated JW18 infection frequency + 3 SD. To enable comparison of hits identified on different treatment plates, the scaling of this initial hit range was next reset to span from 0 to 1, thus applying a uniform, normalized hit range to all plates. To further increase the stringency for identifying hits, we also calculated an average infection frequency for all JW18 cells on the plate (treated or not), as most treatment wells are expected to be indistinguishable from untreated controls. Wells that lay within 3 SD of the mean were excluded from the hit list. Hit wells identified in only one of two replicates were also removed.

Ubiquitin foci staining and quantification

For analysis of ubiquitin foci in tissue culture cells, chamber slides were coated with 0.5 mg/ml Concanavalin A, followed by addition of JW18 cells. After a 24-hr incubation at 25°, cells were fixed for 20 min in 4% formaldehyde, blocked using 1% BSA, and stained with anti-ubiquitin [Enzo Mono- and Poly-ubiquitinylated Conjugates (FK2) BML-PW8805] for 1 hr at 1:100 dilution. Goat anti-mouse Alexa 594 (Invitrogen) was used at a 1:1250 dilution in PBS/0.1% Triton. Cells were imaged on a Leica DMI6000B wide-field inverted microscope equipped with a Hamamatsu EM CCD camera (ORCA C9100-02) at ×100 magnification. Areas to image were selected randomly without bias. Foci were quantified by eye from cells with all boundaries visible in the image. Chi-squared analysis in SPSS was used to determine significance, and *post hoc* tests performed as previously described (Beasley and Schumacker 1995).

For analysis of ubiquitin foci in *D. melanogaster* oogenesis, flies of the genotype *w*; *Sp/Cyo*; *Sb/TM6B* were reared on fly food consisting of 0.5% agar, 7% molasses, 6% cornmeal, and 0.8% killed yeast. Newly eclosed flies were collected and reared for 5 days. Ovaries were dissected in EBR (Ringer's solution) and fixed for 5 min in 600 μl heptane and 100 μl devitellinizing solution (100 μl Buffer B, 112.5 μl 32% paraformaldehyde, and 387.5 μl of diH_2O) (Verheyen and Cooley 1994). Ovaries were then rinsed, treated with RNAse overnight, blocked with 1% BSA, and incubated with anti-ubiquitin [Enzo Mono- and Poly-ubiquitinylated Conjugates (FK2) BML-PW8805] overnight at a 1:50 dilution. Last, the ovaries were incubated with goat anti-mouse:Alexa 488 at a 1:500 dilution and resuspended overnight in mounting media containing propidium iodide (PI). All samples were then imaged on a Leica SP2 confocal microscope at ×63 magnification with ×1.5 zoom. Experimental samples verified to exhibit the same degree of compression as the control sample were pursued further, while any experimental samples deviating from that were discarded. Z-series images were acquired from oocytes at 1.5-μm intervals. Uniform intensity settings were applied to all egg chambers imaged within each replicate. A minimum of 7–10 oocytes were ultimately imaged from each condition per replicate with all experimental oocytes matched for morphological consistency against control oocytes of the same replicate. Significance was determined by ANOVA.

Drug treatments in Drosophila

Newly eclosed flies of the genotype *w*; *Sp/Cyo*; *Sb/TM6B* were collected, reared for 2 days, and then exposed to food containing compounds of interest for 3 days. Drugs were diluted to a final concentration of 100 μM in food. Equivalent amounts of carrier DMSO diluted into these nutrient sources were used as a control.

Generation of Wolbachia-infected RNAi lines in Drosophila

*w*Mel *Wolbachia* were crossed from *w*; *Sp/Cyo*; *Sb/TM6B* into a germline triple driver stock (Mazzalupo and Cooley 2006) to ultimately generate infected flies of the genotype *w*; *P{GAL4-Nos.NGT}40*; *P{GAL4::VP16-Nos.UTR}MVD1* (Serbus *et al.* 2015). Females from this infected driver stock were then crossed to males from responder stocks that carried the following upstream activation sequence (UAS) dsRNA transgenes: the *Ubc6* Valium20 TRiP line: *y,v*; *P{TRiP.HMS02466}attP40*; the *psGEF* Valium20 TRiP line: *y, sc,v*; *P{TRiP.HMS00320}attP2*; the *mtt* Valium20 TRiP line: *y,sc,v*; *P{TRiP.HMS00367}attP2*; the *ND-B17.2* Valium20 line: *y,sc,v*; *P{TRiP.HMS01584}attP2*; and the CG18324 Valium20 line: *y,sc,v*; *P{TRiP.HMS01199}attP2/TM3*, *Sb*. *Wolbachia*-infected driver females were also outcrossed to OreR uninfected males in parallel for analysis as a control.

Quantification of Wolbachia nucleoids in oogenesis

PI staining of *Drosophila* ovarian tissue was done using established methods (Serbus *et al.* 2012). Data collection was

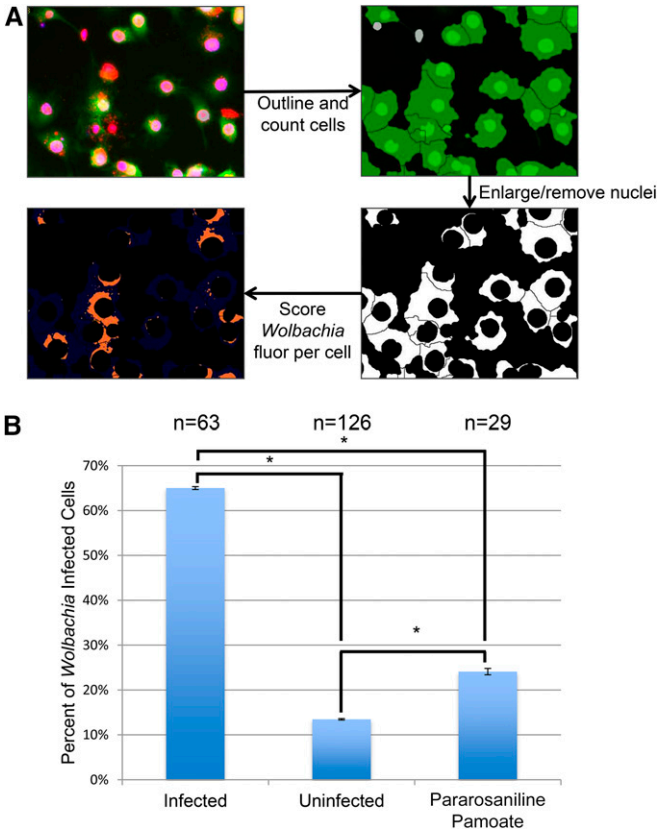

Figure 1 Automated microscope-based quantification of *Wolbachia* titer. (A) Flow chart showing screening methodology. Top left panel: *Wolbachia*-infected JW18 cells showing fluorescence from the markers DAPI (blue) and anti-histone (red), and the GFP-Jupiter (green). Top right panel: The journaling algorithm outlines cell borders based upon Jupiter-GFP. Bottom right panel: The algorithm digitally removes the nucleus from each cell based upon anti-histone staining. Bottom left panel: The total cytoplasmic DAPI signal in each cell is scored. (B) Graph depicts the percentage of cells scored by this algorithm as "*Wolbachia*-infected" in control JW18 cells, cured JW18 cells, and pararosaniline pamoate-treated JW18 cells. Though the algorithm can mis-identify fluorescent debris in the well as "infected cells," there are consistent significant differences by ANOVA between all of the control conditions tested ($P < 0.0001$). Error bars represent the SEM.

conducted as previously. All tissues were imaged using a Leica SP2 confocal microscope. *Wolbachia* were quantified in single focal planes of stage 10 oocytes using established methods (Serbus *et al.* 2015). Average *Wolbachia* titer values associated with drug treatments were normalized against their respective DMSO controls as previously to ensure comparability between experiments in displays of the data (Serbus *et al.* 2015). Statistical analysis was conducted on raw data only using ANOVA, as described previously (Serbus *et al.* 2012). A minimum of 2–3 experimental replicates were performed for the germline staining experiments described in this study.

Transmission electron microscopy

LDW1 cells and the cured equivalent LDW1DOX were fixed with 2% glutaraldehyde and 0.5% paraformaldehyde in Cacodylate buffer 0.075M and postfixed with 2% osmium tetroxide. Samples were dehydrated through a graded series of ethanol and embedded in epoxy resin. Ultrathin (70 nm) sections (Ultracut UC6, Leica) were collected on formvar/carbon-coated copper grids. Sections were then poststained by aqueous 4% uranyl acetate and lead citrate. All samples were observed in a Tecnai12 (FEI, The Netherlands) transmission electron microscope at 80 kV equipped with a 1K×1K Keen View camera. Chi-square analysis was used to determine significance, with *post hoc* tests performed as previously (Beasley and Schumacker 1995).

Data availability

All primary data can be found in Supplemental Material, File S1. Additional information about *in vivo* validation of genes that alter *Wolbachia* quantity can be found in Figure S1.

Results

A genome-wide RNAi cell-based screen yields host genes that either enhance or suppress Wolbachia titer

To identify host components that influence *Wolbachia* infection of insect cells, we took advantage of the ability to perform genome-wide RNAi screens in *Drosophila* tissue culture cells. Because *Drosophila* cell lines are particularly amenable to RNAi-based screening, this approach has been successfully used for studying a number of cellular processes including the cellular basis of host–pathogen interactions (Moser *et al.* 2010). Here we used a well-characterized *Wolbachia*-infected cell line known as JW18 (Serbus *et al.* 2012). Our analysis revealed that 90% of the JW18 host cells are infected and *Wolbachia* have no obvious effects on cell viability or division (Serbus *et al.* 2012). Quantification of *Wolbachia* infection was based on fluorescent images of *Wolbachia*-infected and cured JW18 cell lines using automated microscopy and journaling software (Figure 1).

By using the JW18 cell line in the 384-well plate format, we screened an RNAi library that targets 15,699 *Drosophila* protein-encoded genes (Goshima *et al.* 2007). *Wolbachia*-infected JW18 cells were plated into individual wells, each containing a unique dsRNA, and allowed to incubate for 5 days. Robotics and automated microscopy were used to fix, stain, and image the cells (see *Materials and Methods*). The JW18 cell line expresses a GFP-Jupiter fusion protein that labels the cytoskeleton (Karpova *et al.* 2006), thus highlighting the entire cytoplasm and indicating cell boundaries. Anti-histone staining labeled the host nuclei, and DAPI was used to stain both host nuclei and cytoplasmic *Wolbachia*. Through customized journaling software, the overlap of anti-histone and DAPI nuclear staining enabled digital removal of the nucleus. This facilitated quantification of cytoplasmic DAPI, representing *Wolbachia* density per cell (Figure 1) (Serbus *et al.* 2012). Each cell was scored as *Wolbachia* positive or negative based on a predetermined cytoplasmic DAPI intensity cut-off value. Ten images per well were recorded and analyzed, and two independent screens of the RNAi library were performed. RNAi knockdowns that significantly reduced or increased the proportion of *Wolbachia*-infected cells per well without

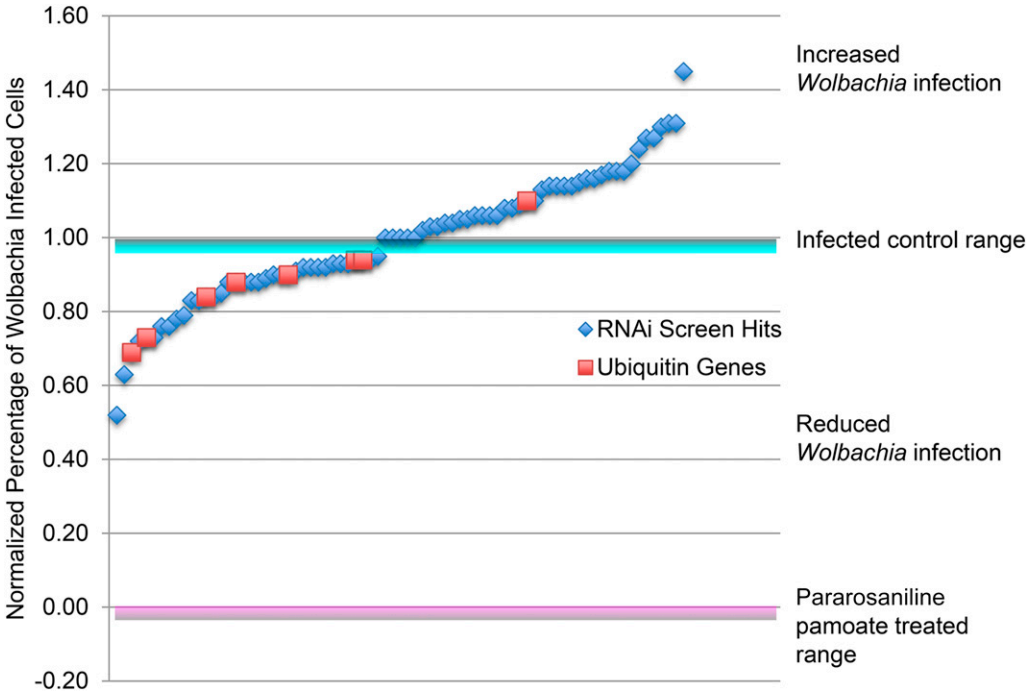

Figure 2 RNAi knockdowns that decreased or increased *Wolbachia* infection rate. Of 15,699 transcribed host genes, 36 candidate genes were identified that dramatically reduced *Wolbachia* titer and 41 that increased *Wolbachia* titer when knocked down via RNAi. Blue diamonds below or above the infected control range indicates dsRNA treatments targeting a single host gene that reduced or increased the proportion of *Wolbachia*-infected tissue culture cells. Red boxes indicate ubiquitin-related dsRNA treatment outcomes.

dramatically altering cell viability in both independent replicates were scored as hits (Figure 2). Because we are starting with a population in which 90% or more of the cells are infected, RNAi-induced alterations in the ability of *Wolbachia* to infect cells are expected to exert only a minor impact on titer.

The screen yielded 36 host genes that when knocked down through RNAi resulted in a significant drop in *Wolbachia* titer. These included hits in two genes involved in host lipid metabolism: CG9243, a phospholipase D; and CG1718, a gene involved in sterol uptake and esterification. In addition, hits in three mitochondrial metabolism components were recovered: CG3214, an NADH dehydrogenase; CG14757, a succinate dehydrogenase; and CG18324, a mitochondrial transporter. Knockdown of host genes encoding ATPases, GTPases, and ribosomal proteins also reduced titer (Table 1 and Table 2).

Particularly striking, the screen yielded eight hits in the ubiquitin-related pathways, seven of which reduced the proportion of *Wolbachia*-infected tissue culture cells. DsRNA targeting the Ubiquitin-60S ribosomal protein L40 (CG2960), lingerer (CG8715), Ubiquitin-5E (CG32744), the ubiquitin transferase mei-P26 (CG12218), Ubiquitin-like protein 5 (CG3450), Ubiquitin-conjugating enzyme Ubc6 (CG2013), and Ubiquitin-like protein (CG12725) reduced infection, and targeting of the ubiquitin transferase CG31807 increased infection (Table 1 and Table 3). Ubiquitin is a small protein with a variety of functions including the marking of proteins for degradation and is targeted by a number of intracellular bacteria (Zhou and Zhu 2015). Previous inspection of the *Wolbachia* genome revealed that *Wolbachia* lack the ability to synthesize key amino acids and thus rely on the host as a source (Wu *et al.* 2004; Foster *et al.* 2005). Thus, it is possible that *Wolbachia* require high levels of host proteolysis to supply sufficient amino acids for growth and reproduction.

The RNAi screen also yielded 41 host genes that when knocked down significantly increased the proportion of *Wolbachia*-infected cells. These included hits in: CG4484, a sucrose transporter; CG30361, a G-protein-coupled receptor; CG1657, a GTPase-activating protein (GAP); CG7968, a hemolymph juvenile hormone-binding protein. Of the 41 hits that increased *Wolbachia* titer, 32 were of unknown function. Unlike the hits that reduced titer, we did not recover multiple hits in known specific biological processes or pathways (Table 3).

The presence of Wolbachia increases the quantity and distribution of ubiquitinated proteins in infected host cells and oocytes

Given RNAi knockdowns of host components involved in the ubiquitin/proteolysis pathway resulted in a reduction in *Wolbachia* titer, we examined whether the presence of *Wolbachia* might influence the ubiquitination state of host proteins. This was accomplished through immunofluorescence analysis with an antibody that specifically recognizes ubiquitin-conjugated host proteins. The antibodies were developed to recognize the multi-ubiquitinated chains of polyubiquitinated proteins but not free ubiquitin (see *Materials and Methods*) (Fujimuro *et al.* 1994; Everett 2000). This analysis revealed a significant increase in the number of ubiquitin foci in the *Wolbachia*-infected cells compared to the uninfected controls (Figure 3). Figure 3B presents DAPI-stained nuclei (blue), microtubule-labeled cytoplasm (green), and ubiquitin foci (red) in JW18 infected and uninfected cells. The images reveal that the number, size, and intensity of the ubiquitin foci are much greater in the former. For

Table 1 List of host genes that reduce *Wolbachia* infection rates when knocked down

CG#	Effect on titer	Gene name	Normalized value	Functional category	Additional functional category
CG14835	Reduced	CG14835	0.52		
HDC10201	Reduced	HDC10201	0.63		
CG12725	Reduced	CG12725	0.69	Ubiquitin	
CG9777	Reduced	CG9777	0.72		
CG12218	Reduced	mei-P26	0.73	Ubiquitin transferase	Ligase
HDC05374	Reduced	HDC05374	0.73		
CG1527	Reduced	RpS14b	0.76	Ribosomal	
CG14579	Reduced	CG14579	0.76		
CG10970	Reduced	CG10970	0.78	Acylphosphatase	
CG13738	Reduced	CG13738	0.79		
CG2916	Reduced	Sep5	0.83	Septin	GTP-binding protein
CG14047	Reduced	PsGEF	0.83	RhoGEF	GTPase
CG2960	Reduced	RpL40	0.84	Ubiquitin	Ribosomal
CG32100	Reduced	CG32100	0.84		
CG30372	Reduced	Asap	0.85	ArfGap	GTPase activator
CG2958	Reduced	lectin-24Dd	0.88	C-type lectin	Carbohydrate binding
CG3450	Reduced	ubl	0.88	Ubiquitin	
CG4688	Reduced	GstE14	0.88	Glutathione S-transferase	
CG32399	Reduced	CG32399	0.88		
CG7320	Reduced	CG7320	0.88	Hemocyanin	
CG12172	Reduced	Spn43Aa	0.89	Serpin	Endopeptidase inhibitor
CG1344	Reduced	CG1344	0.90	Kinase	
CG3214	Reduced	ND-B17.2	0.90	Mitochondrial	NADH dehydrogenase
CG2013	Reduced	Ubc6	0.90	Ubiquitin	Ubiquitin-conjugating enzyme
HDC15882	Reduced	HDC15882	0.91		
CG33196	Reduced	dpy	0.92	EGF domain	Structural constituent
CG18324	Reduced	CG18324	0.92	Mitochondrial carrier	Transport
CG14757	Reduced	CG14757	0.92	Mitochondrial	Succinate dehydrogenase
CG12807	Reduced	Spn85F	0.92	Serpin	Endopeptidase inhibitor
CG1070	Reduced	Alh	0.93	Transcription	
CG1332	Reduced	CG1332	0.93	Endocytosis	
CG1718	Reduced	CG1718	0.93	ABC transporter	ATPase
CG8715	Reduced	lig	0.94	Ubiquitin	
CG32744	Reduced	Ubiquitin-5E	0.94	Ubiquitin	
CG1394	Reduced	CG1394	0.94		
CG43345	Reduced	CG43345	0.95	Phospholipase D	Catalytic activity

Hits are ordered from strongest at the top to weakest at the bottom.

example, 85% ($n = 142$) of the infected cells had one or more ubiquitin foci compared to 45% ($n = 138$) for the uninfected cells. Additionally, 51% of infected cells had five or more ubiquitin foci ($n = 72$), which was significantly different ($P = 0.0001$) compared to 7% of uninfected cells with that outcome ($n = 10$) (Figure 3A). Significance was determined using chi-square analysis.

We also performed this analysis on infected and uninfected *Drosophila* oocytes. The images shown in Figure 4 depict oocytes from infected and uninfected adult *D. melanogaster* females. PI (red) stains host nuclei in uninfected cells and both the host nuclei and *Wolbachia* in infected cells. The anti-ubiquitin antibody (green in top panels and black-and-white in bottom panels) stains the ubiquitin foci. Quantification was performed as previously described (Serbus *et al.* 2015) (see also *Materials and Methods*). Ubiquitin foci counts were accomplished by selecting a defined area at the posterior pole from an image of a medial section of each oocyte. This revealed an average of 10 ± 3 ($n = 10$) posterior ubiquitin foci in infected oocytes, in contrast to 3 ± 1 ($n = 10$) posterior ubiquitin foci detected in uninfected oocytes.

Drug-induced inhibition of the proteasome reduces Wolbachia titer in the Drosophila oocyte

To determine if the maintenance of *Wolbachia* titer relies on high levels of host proteasome activity, *Wolbachia*-infected *Drosophila* females were treated with Lactacystin, a proteasome inhibitor that targets the 20S subunit of the proteasome (Yang *et al.* 2008). After being kept on a regular diet for 2 days, the flies were exposed to food containing 100 μM lactacystin for 3 days. Control females were exposed to food with an equivalent amount of carrier DMSO. Ovarian tissues were dissected and stained with PI to label *Wolbachia* DNA. As previously described, *Wolbachia* abundance was determined by confocal imaging of the medial plane of PI-stained stage 10 oocytes (Serbus *et al.* 2015) (see also *Materials and Methods*). In these images, the PI stains the nuclei of the host follicle cells that border the oocyte and the *Wolbachia* nucleoids within the oocyte (Figure 5). This analysis indicated significant reduction in *Wolbachia* titer in lactacystin-treated oocytes compared to untreated control oocytes (Figure 5, A and B). Control oocytes averaged 700 ± 54 *Wolbachia* ($n = 29$), while the treated oocytes

Table 2 List of host genes that significantly alter *Wolbachia* infection rates ordered by function

	CG#	Effect on titer	Gene name	Normalized value	Functional category	Additional Functional Category
ATP/GTP	CG1718	Reduced	CG1718	0.93	ABC transporter	ATPase
	CG30372	Reduced	Asap	0.85	ArfGap	GTPase activator
	CG14047	Reduced	PsGEF	0.83	RhoGEF	GTPase
	CG2916	Reduced	Sep5	0.83	Septin	GTP-binding protein
	CG1657	Increased	CG1657	1.20	GTPase activating	Activates Rab GTPases
Kinase	CG1344	Reduced	CG1344	0.90	Kinase	
	CG5813	Increased	chif	1.14	Kinase	DBF zinc finger
Mitochondrial	CG3214	Reduced	ND-B17.2	0.90	Mitochondrial	NADH dehydrogenase
	CG14757	Reduced	CG14757	0.92	Mitochondrial	Succinate dehydrogenase
	CG18324	Reduced	CG18324	0.92	Mitochondrial carrier	Transport
Ribosomal	CG2960	Reduced	RpL40	0.84	Ubiquitin	Ribosomal
	CG1527	Reduced	RpS14b	0.76	Ribosomal	
Serpin	CG12172	Reduced	Spn43Aa	0.89	Serpin	Endopeptidase inhibitor
	CG12807	Reduced	Spn85F	0.92	Serpin	Endopeptidase inhibitor
Ubiquitin	CG2960	Reduced	RpL40	0.84	Ubiquitin	Ribosomal
	CG8715	Reduced	lig	0.94	Ubiquitin	
	CG32744	Reduced	Ubiquitin-5E	0.94	Ubiquitin	
	CG3450	Reduced	ubl	0.88	Ubiquitin	
	CG2013	Reduced	Ubc6	0.90	Ubiquitin	Ubiquitin-conjugating enzyme
	CG12725	Reduced	CG12725	0.69	Ubiquitin	
	CG12218	Reduced	mei-P26	0.73	Ubiquitin transferase	Ligase
	CG31807	Increased	CG31807	1.10	Ubiquitin transferase	RING finger domain
Ungrouped	CG10970	Reduced	CG10970	0.78	Acylphosphatase	
	CG1629	Increased	mal	1.04	Aminotransferase	MOSC domain
	CG2958	Reduced	lectin-24Dd	0.88	C-type lectin	Carbohydrate binding
	CG33196	Reduced	dpy	0.92	EGF domain	Structural constituent
	CG1332	Reduced	CG1332	0.93	Endocytosis	
	CG30361	Increased	mtt	1.31	G-protein-coupled receptor	
	CG4688	Reduced	GstE14	0.88	Glutathione S-transferase	
	CG7968	Increased	CG7968	1.03	Hemolymph juvenile hormone-binding protein	
	CG7320	Reduced	CG7320	0.88	Hemocyanin	
	CG32005	Increased	CG32005	1.14	High-Mobility group box	DNA binding
	CG43345	Reduced	CG43345	0.95	Phospholipase D	Catalytic activity
	CG7988	Increased	CG7988	1.30	Regulation of circadian clock	
	CG4484	Increased	Slc45-1	1.45	Sucrose transporter	
	CG1070	Reduced	Alh	0.93	Transcription	

averaged 534 ± 35.0 ($n = 29$) ($P = 0.012$). Significance was determined using ANOVA.

RNAi knockdown of proteasome component Ubc6 results in a dramatic decrease in Wolbachia titer in the oocyte

We next genetically tested the impact of the host ubiquitin/proteasome pathway on oocyte *Wolbachia* titer. We used the GAL4:UAS system to knockdown specific components of the ubiquitin/proteasome pathway in the female germline (see *Materials and Methods*) (Hudson and Cooley 2014). Because *Wolbachia* is intimately associated with the ER in our cell lines (see next section), we focused on the host factor Ubc6 recovered in our screen (Table 1). Ubc6 is an ER integral membrane protein that functions as an E2 conjugating enzyme in the ERAD pathway: endoplasmic reticulum (ER)-associated degradation of mis-folded proteins (Lemus and Goder 2014). Ubc6 is specifically required for the degradation of cytosolic domains of membrane proteins (ERAD-C) (Metzger *et al.* 2008). Previous studies have successfully knocked down Ubc6 using UAS Ubc6 RNAi fly lines (Ashton-Beaucage *et al.* 2016). By crossing in the maternal nanos-GAL4 driver into the UAS-Ubc6 RNAi line, we specifically knocked down the level of Ubc6 in *Drosophila* female germline cells. This RNAi knockdown of Ubc6 in the *Drosophila* germline resulted in an approximately fourfold reduction in oocyte *Wolbachia* titer (Figure 5). The wild-type oocytes averaged 368 ±133 ($n = 19$) *Wolbachia* while the Ubc6 knockdowns averaged 93 ± 43 ($n = 19$) ($P < 0.01$) (Figure 5). These results suggest that a fully functional host ERAD pathway is required to maintain *Wolbachia* titer in the *Drosophila* oocytes and cell lines.

Wolbachia is closely associated with and alters the morphology of the ER

Given the dependence of *Wolbachia* titer on ERAD, we performed ultrastructural analysis on the *Wolbachia*-infected cell lines to determine its subcellular localization. Ultrastructural images of the *Wolbachia*-infected cell line are shown in Figure 6 and Figure 7. The *Drosophila* cells are round with a

Table 3 List of host genes that increase *Wolbachia* infection rates when knocked down

CG#	Effect on titer	Gene name	Normalized value	Functional category	Additional functional category
CG10589	Increased	CG10589	1.00	Domain of unknown function	
CG11231	Increased	CG11231	1.00		
CG14442	Increased	CG14442	1.00		
CG32736	Increased	CG32736	1.00	Uncharacterized protein family	
CG32718	Increased	CG32718	1.00		
CG15480	Increased	CG15480	1.02		
CG7968	Increased	CG7968	1.03	Hemolymph juvenile hormone-binding protein	
HDC17458	Increased	HDC17458	1.03		
CG1629	Increased	mal	1.04	Aminotransferase	MOSC domain
CG34434	Increased	CG34434	1.04		
CG1971	Increased	CG1971	1.05		
HDC16920	Increased	HDC16920	1.05		
CG18656	Increased	CG18656	1.06		
CG4455	Increased	CG4455	1.06		
CG4631	Increased	CG4631	1.06	Domain of unknown function	
CG11260	Increased	CG11260	1.06		
CG32790	Increased	CG32790	1.08		
CG3568	Increased	CG3568	1.08	Domain of unknown function	
CG18404	Increased	CG18404	1.09		
CG31807	Increased	CG31807	1.10	Ubiquitin transferase	RING finger domain
CG43117	Increased	CG43117	1.10		
CG14673	Increased	CG14673	1.13		
CG5813	Increased	chif	1.14	Kinase	DBF zinc finger
CG32005	Increased	CG32005	1.14	High-mobility group box	DNA binding
HDC12508	Increased	HDC12508	1.14		
HDC12757	Increased	HDC12757	1.14		
HDC19233	Increased	HDC19233	1.15		
CG9263	Increased	CG9263	1.16		
CG31819	Increased	CG31819	1.16		
CG31817	Increased	CG31817	1.17		
CG32988	Increased	CG32988	1.18		
CG31813	Increased	CG31813	1.18		
CG42749	Increased	CG42749	1.18		
CG1657	Increased	CG1657	1.20	GTPase activating	Activates Rab GTPases
CG16852	Increased	CG16852	1.24		
CG4666	Increased	CG4666	1.27		
CG13365	Increased	CG13365	1.27		
CG7988	Increased	CG7988	1.30	Regulation of circadian clock	
CG30361	Increased	mtt	1.31	G-protein-coupled receptor	
CG16853	Increased	CG16853	1.31		
CG4484	Increased	Slc45-1	1.45	Sucrose transporter	

Strongest to weakest hits are ordered from top to bottom

mean diameter of 6–8 μm. *Wolbachia* (W), golgi (G), the endoplasmic reticulum cisternae (ERC), mitochondria (M), and nuclei (N) are readily visualized in these cells (Figure 6, A and B). *Wolbachia* tend to exhibit an approximate diameter of 0.5 μm and occasionally observe lengths >1 μm (Figure 6C). As previously described, *Wolbachia* are often encompassed by a double membrane, enclosing the bacteria within a small vacuole (Voronin *et al.* 2004; Chagas-Moutinho *et al.* 2015). In some instances, multiple *Wolbachia* occupy the same vacuole. Dividing *Wolbachia* are depicted in Figure 6D. In this case, both daughter bacteria lie in the same vacuole although it is expected that each daughter bacterium will reside within its own host vacuole after completion of division (Figure 6D).

Our ultrastructural analysis reveals an intimate association between *Wolbachia* and the host ER. Figure 7A depicts an elaboration of the ER extending from the nuclear envelope to a *Wolbachia* located in the cytoplasm. Figure 7, B and C depict similar ER extensions that encompass individual *Wolbachia*. In some instances, there is a direct contact and continuity between the host ER and *Wolbachia* membrane vacuole. This is especially evident in Figure 7D. These images suggest that *Wolbachia* are connected to the luminal space of the ER.

In addition to the intimate association between *Wolbachia* and the ER, we find that the presence of *Wolbachia* induces dramatic alterations in ER morphology. In the uninfected cell line, the ER exhibits classic tubule morphology with ribosomes decorating its entire length (Figure 8, A and B). By contrast, in the *Wolbachia*-infected cells, the ER is highly elaborated forming a complex network of extensions

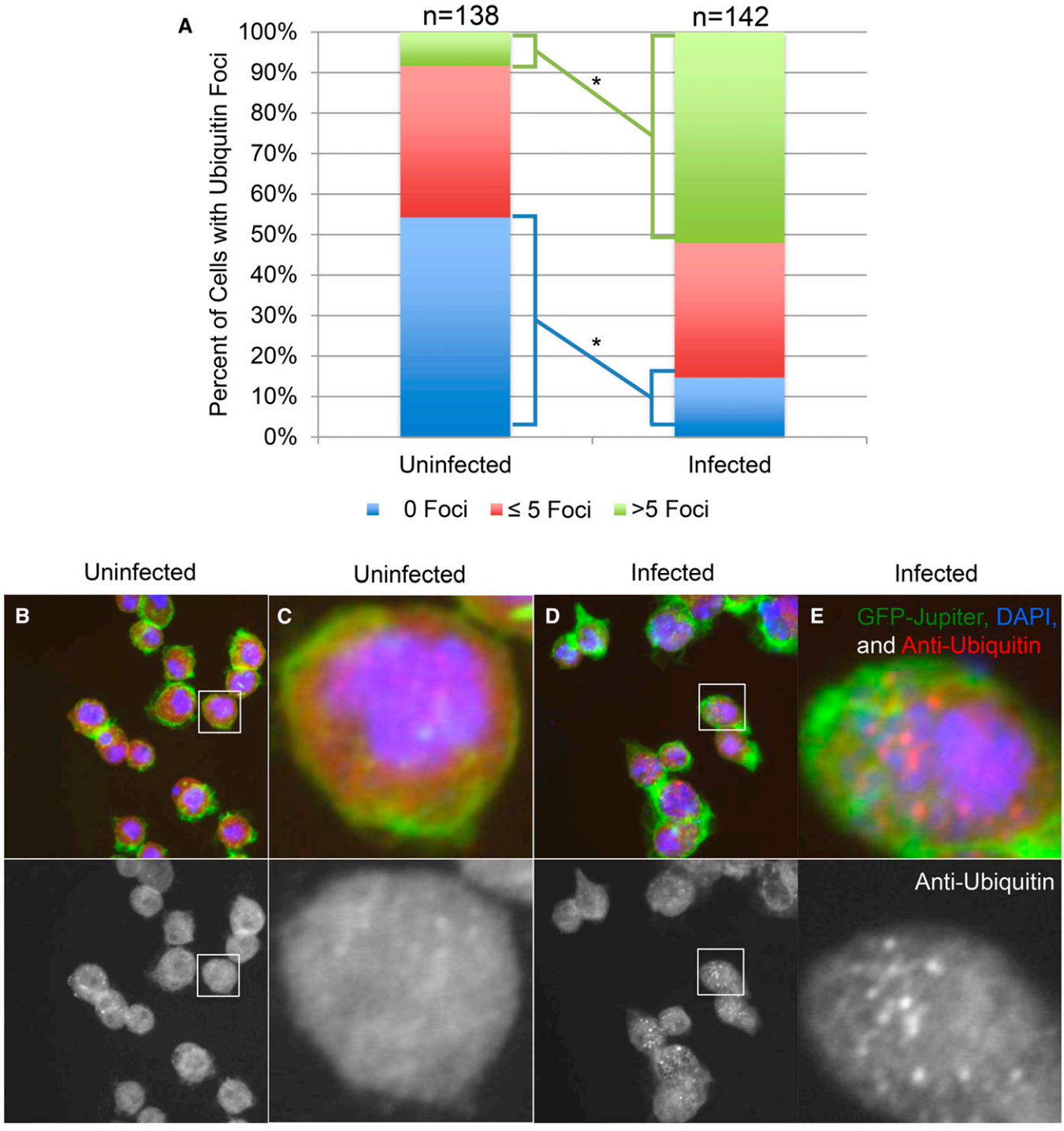

Figure 3 Increase in ubiquitin foci in *Wolbachia*-infected tissue culture cells. (A) Quantification of the number of ubiquitin foci in infected and uninfected cells. All *P* values were below 0.0001, and adjusted α value was 0083333. (B and C) Low and high magnification images of stained uninfected cells. (D and E) Low and high magnification images of stained *Wolbachia*-infected cells. Staining indicates DNA (blue), microtubules (GFP-Jupiter) (green), and ubiquitin foci (red). Significance was determined using chi-square analysis.

(Figure 8, C and D). In addition, the ER tubules have expanded to form large cisternae. As seen in the images, *Wolbachia* are often associated with these cisternae. To quantify the effect of *Wolbachia* on ER morphology, we analyzed randomly selected EM images from *Wolbachia*-infected and cured cell lines (n = 128 and 121, respectively) (Figure 9). Quantification revealed a dramatic increase in all classes of abnormal ER morphology, including the ER network extensions, ER swelling, and formation of large ER cisternae. Particularly striking is the 10-fold increase in the formation of ER cisternae in *Wolbachia*-infected cells (Figure 9).

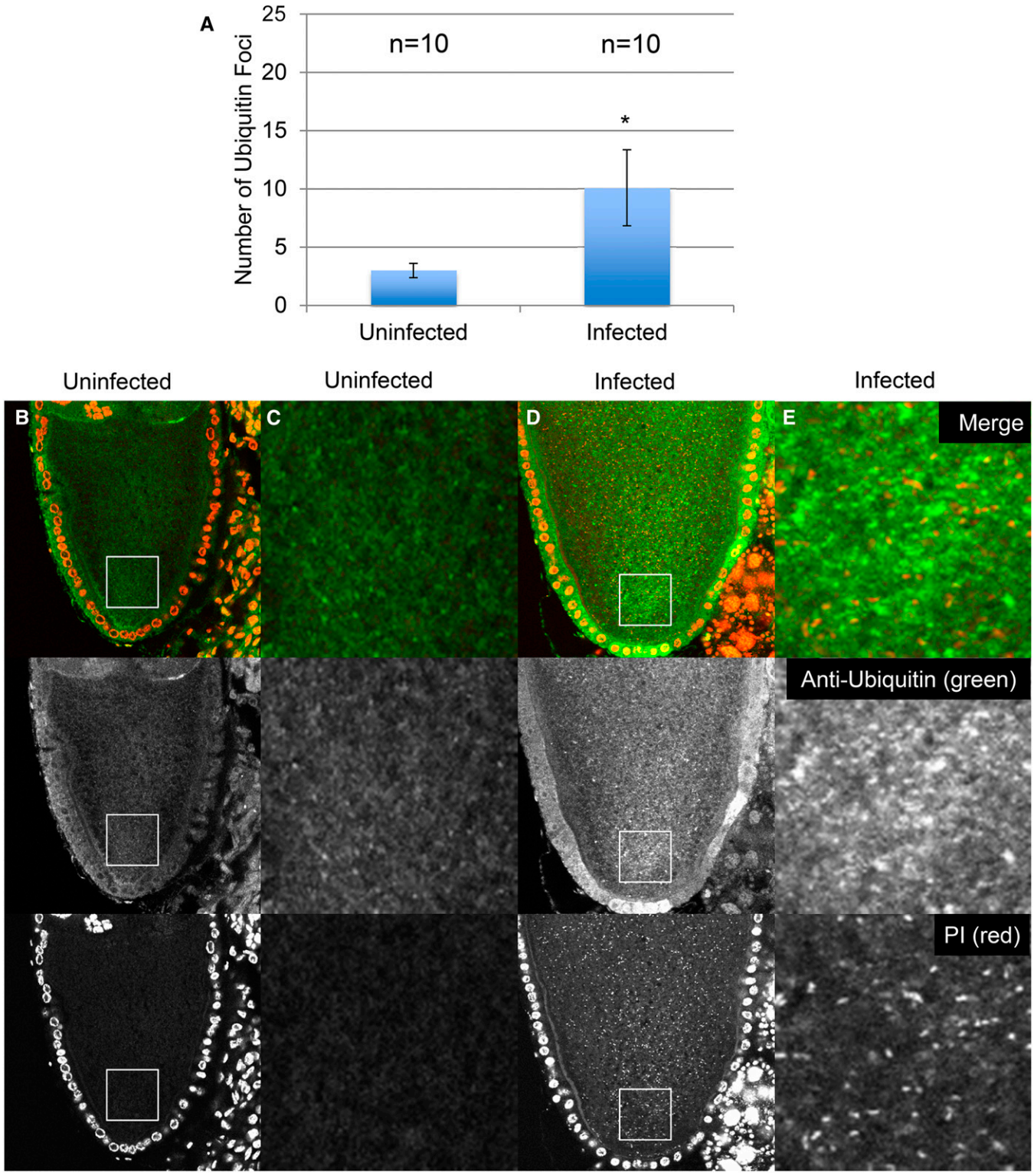

Figure 4 Increase in ubiquitin foci in *Wolbachia*-infected *Drosophila* oocytes. Immmunofluorescence analysis using an anti-ubiquitin antibody indicated more ubiquitin foci in *Wolbachia*-infected oocytes. (A) Quantification of ubiquitin foci per area in medial planes of infected and uninfected oocytes. Average values were significantly different according to ANOVA ($P = 0.046$). Error bars indicate SEM. (B and C) Low and high magnification images of uninfected oocytes. (D and E) Low and high magnification images of *Wolbachia*-infected oocytes. DNA (red) and ubiquitin foci (green).

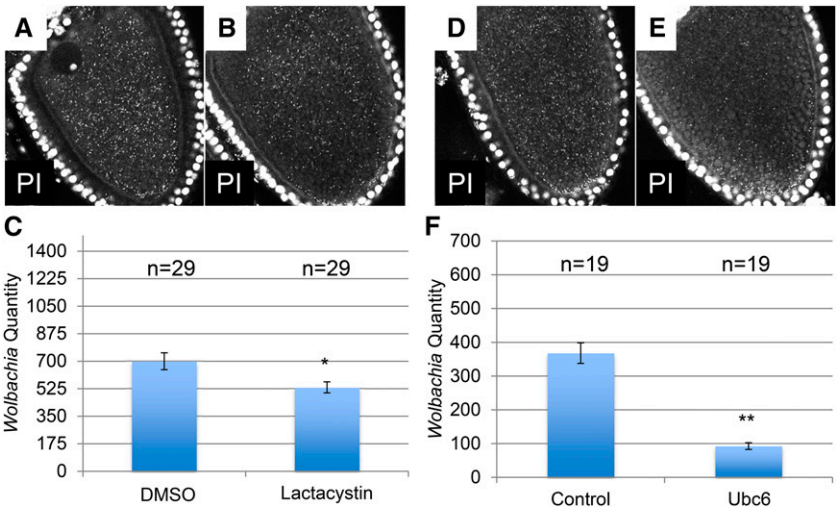

Figure 5 Disruption of host proteasome reduces *Wolbachia* titer in the *Drosophila* oocyte. Adult females were fed food containing either DMSO (A) or lactacystin (B). (C) Quantification of the *Wolbachia* in medial plane of stage 10 oocytes indicated a significant difference by ANOVA ($P = 0.012$). Control (D) and *Ubc6* (E) knocked down using GAL4-UAS dsRNA expression. Quantification of oocyte titers (F) indicated a significant difference by ANOVA ($P < 0.001$). Error bars indicate SEM.

Discussion

Performing the genome-wide, cell-based RNAi screen enabled us to comprehensively identify host factors that influenced *Wolbachia* titer. Of the 15,699 targets tested by RNAi disruption (Goshima *et al.* 2007), the screen yielded 36 RNAi treatments that decreased *Wolbachia* titer and 41 RNAi treatments that increased titer, implicating 77 host genes. The fact that only a small fraction of the RNAi knockdowns influenced titer suggests that *Wolbachia* possesses robust mechanisms of maintaining specific intracellular titers. Not surprisingly, hits that reduced *Wolbachia* titer spanned a broad array of cellular functions including host transcriptional and translational machinery, mitochondrial proteins, cell signaling, and metabolism (Table 1).

Of the 77 gene knockdowns that significantly altered *Wolbachia* titer, eight genes were involved in the ubiquitin/proteolysis pathway. These included *RpL40*, *lig*, *Ubiquitin-5E*, *ubl*, *Ubc6*, *mei-P26*, *CG12725*, and *CG31807*. These studies indicate that maintenance of *Wolbachia* titer requires fully functional host ubiquitin and proteolysis pathways. A likely explanation for this dependence comes from genomic studies demonstrating that *Wolbachia* lacks many of the pathways for amino acid production (Wu *et al.* 2004; Brownlie and O'Neill 2005). A robust ubiquitin/proteasome pathway would ensure an adequate pool of amino acids in order for *Wolbachia* to thrive. Similarly, RNAi screens in *Drosophila* infected with *L. monocytogenes*, *M. fortuitum*, and *F. tularensis* revealed that bacteria titer uptake and proliferation was highly dependent on the ubiquitin and proteasome pathways (Agaisse *et al.* 2005; Philips *et al.* 2005; Akimana 2010).

We used immunofluorescence to determine if the presence of *Wolbachia* influenced the ubiquitination state of proteins in these cells by taking advantage of an antibody that broadly recognizes mono and poly-ubiquitinated proteins (Everett 2000). Our analysis of ubiquitin staining in tissue culture cells and *Drosophila* oogenesis revealed significantly more foci in the *Wolbachia*-infected conditions than uninfected conditions. Previous studies using an antibody that broadly recognizes poly-ubiquitinated proteins revealed that the herpes simplex virus immediate-early protein ICPO induces proteasome-dependent degradation of host proteins and results in a similar increase in the number and extent of ubiquitin foci, which are interpreted as sites of concentrated poly-ubiquitinated proteins (Everett 2000).

Function disruption tests also support a role for the ubiquitin-proteasome system in regulating *Wolbachia* titer in *Drosophila* oogenesis. Disruption of proteasome activity with the small molecule inhibitor lactacystin also significantly reduced oocyte *Wolbachia* titer, indicating that maintenance of *Wolbachia* titer in oogenesis is dependent on host proteasome activity. We also knocked down Ubc6, an E2 conjugating enzyme involved in the ERAD pathway (Metzger *et al.* 2008). Ubc6 is specifically associated with the ERAD-C complex that monitors the folding state of the cytosolic domains of membrane proteins. These results suggest that *Wolbachia* preferentially rely on the ERAD-C protein degradation pathway as an amino acid source. In support of this conclusion, our EM analysis of *Wolbachia*-infected tissue culture cells reveals that *Wolbachia* exhibits a particularly close association with the ER (Figure 6, Figure 7, and Figure 8).

Our results are in accord with proteomic and genomic studies indicating that *Wolbachia* in *Aedes* and *B. malayi* must rely on host-derived amino acids (Foster *et al.* 2005; Baldridge *et al.* 2014). In addition, studies demonstrate that amino acids may be limiting because *Wolbachia* competes with its host for amino acids (Caragata et al., 2014). Our findings are also in line with work demonstrating that mosquito cell lines newly infected with *Wolbachia* exhibit up-regulation of the host 26S proteasome and a general increase in ubiquitinated proteins (Fallon and Witthuhn 2009). However, a key difference between these studies in mosquito cells and our work in *Drosophila* is the timeline of the effects. Differences in the proteasome and ubiquitination levels were not observed between long-term *Wolbachia*-infected and cured mosquito cell lines, nor was it observed in cured cell lines reinfected with *Wolbachia*. This suggests that the up-regulation was a transient host response to new infection.

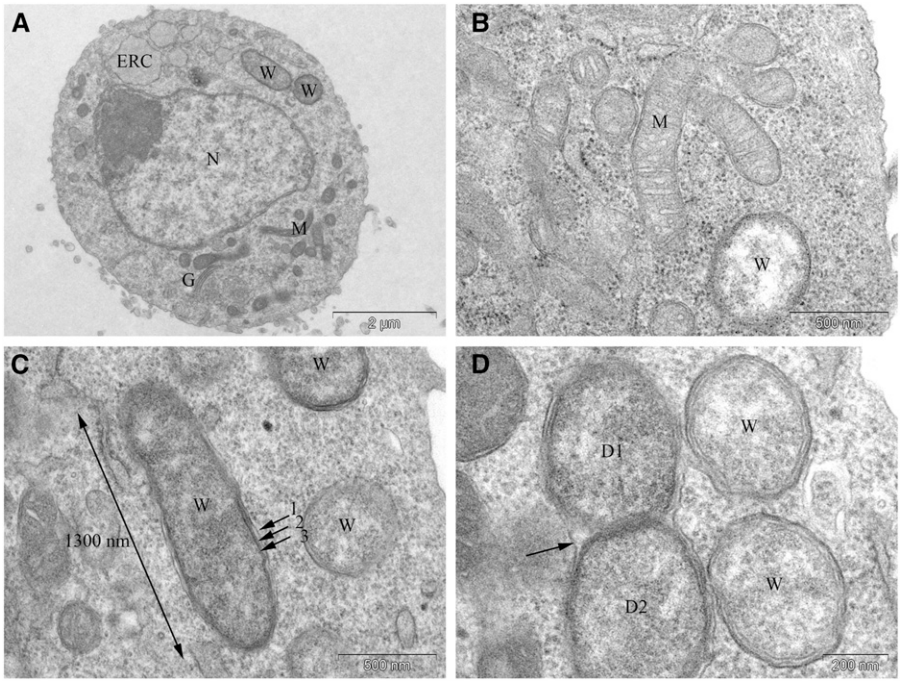

Figure 6 Ultrastructural analysis of *Wolbachia* in *Drosophila* cultured cells. (A) Cross-section of a *Wolbachia*-infected *Drosophila* cell in which the nucleus (N), endoplasmic reticulum cisternae (ERC), golgi (G), mitochondria (M), and *Wolbachia* (W) are readily visualized. Cells are spherical with a mean diameter of 6–8 μm. (B) Mitochondria and *Wolbachia* are readily distinguished as the former exhibit distinct internal tubular structures and are narrower in width. (C) The maximum size observed for *Wolbachia* is a 1300 nm length and 460 nm width. Each *Wolbachia* bacterium is encompassed by three membranes, the outermost derived from the host (arrows 1, 2, 3). (D) Image of dividing *Wolbachia*. The two daughter cells (D1 and D2) lie in the same vacuole (arrow), which ultimately will abscise.

In contrast, we found that up-regulation of the proteasome occurs in *Drosophila* cell lines and oocytes with long-term *Wolbachia* infections. Whether this is the result of a difference in the fundamental biology of mosquito and *Drosophila* cells is unclear.

Our ultrastructural studies of the infected cell lines demonstrate a close association between *Wolbachia* and the ER. As shown in Figure 6 and Figure 7, *Wolbachia* shares membrane with the ER and is often found embedded in the ER. A similar close association between *Wolbachia* and the ER has been documented in early *Drosophila* embryos (Voronin *et al.* 2004), nurse cells (Serbus *et al.* 2011), and in the central nervous system (Strunov and Kiseleva 2014). These observations are intriguing in light of our finding that the ERAD pathway is required for maintaining *Wolbachia* titer both in cells lines and *Drosophila* oocytes. By being embedded in the ER, *Wolbachia* is in prime position to utilize the products derived from ERAD-mediated protein degradation.

An alternative interpretation of these results is based on studies of apicoplasts, organelles present in apicomlexan

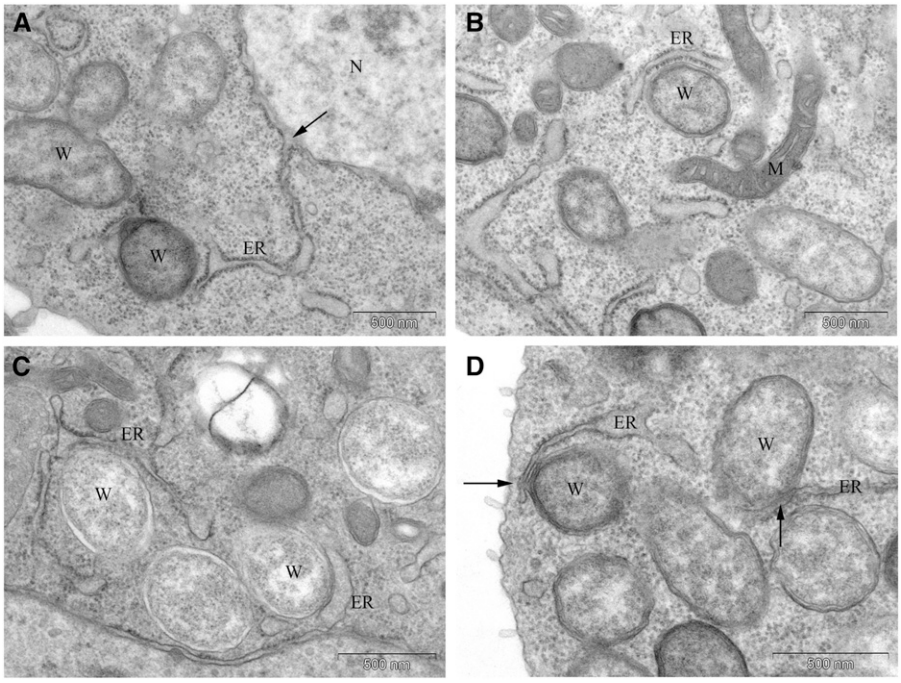

Figure 7 *Wolbachia* closely associate and alter the morphology of the ER. (A) The presence of *Wolbachia* results in an ER extension from the nuclear envelope (arrow) to *Wolbachia*. (B and C) Examples of ER extensions wrapping around and in close association with *Wolbachia*. (D) In some instances, *Wolbachia* appear to communicate with the ER lumen (arrows). W, *Wolbachia*; ER, endoplasmic reticulum; N, nucleus; M, mitochondria.

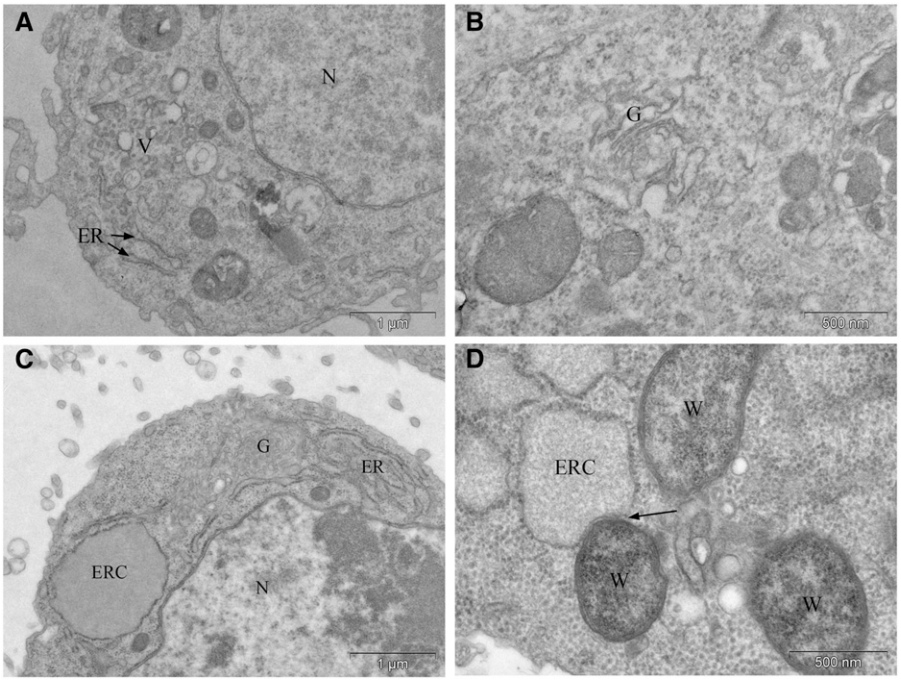

Figure 8 *Wolbachia* alter the morphology of the ER. (A and B) Images from uninfected (doxycycline cured) *Drosophila* cell lines. Under these conditions, the ER compartments exhibited a normal tubular and discrete shape. Additionally, only few Golgi bodies were found. (C and D) Images from *Wolbachia*-infected *Drosophila* cell lines. (C) The presence of *Wolbachia* resulted in the swelling of the ER to form either ER cisternae or a highly elaborate complex of ER extensions and golgi. (D) *Wolbachia* are often observed in close contact with enlarged ER cisternae (ERC, arrow). W, *Wolbachia*; ER, endoplasmic reticulum; N, nucleus; V, vesicles; G, golgi.

parasites including *Toxoplasma gondii* and *Plasmodium falciparum*. This organelle originated from an alga that underwent secondary endocytosis (Vaishnava and Striepen 2006). Apicoplasts have many properties in common with *Wolbachia* including maternal inheritance, multiple membranes, and a close association with the ER (Vaishnava and Striepen 2006). In apicoplasts, the ERAD pathway has been usurped and modified to facilitate import of key required proteins from the host cytoplasm (Agrawal *et al.* 2013). Strikingly, it also relies on the ubiquitin pathway marking proteins for import to the apicoplast. These findings raise the intriguing possibility that *Wolbachia* may also rely on the ERAD pathway for import of host cytoplasmic proteins.

Two other functional categories have been validated *in vivo* in addition to Ubiquitin: "ATP/GTP" and "Mitochondrial." Five hits were identified in the ATP/GTP functional category. We found that knockdown of protostome-specific GEF (CG14047) in the *Drosophila* germline significantly decreased

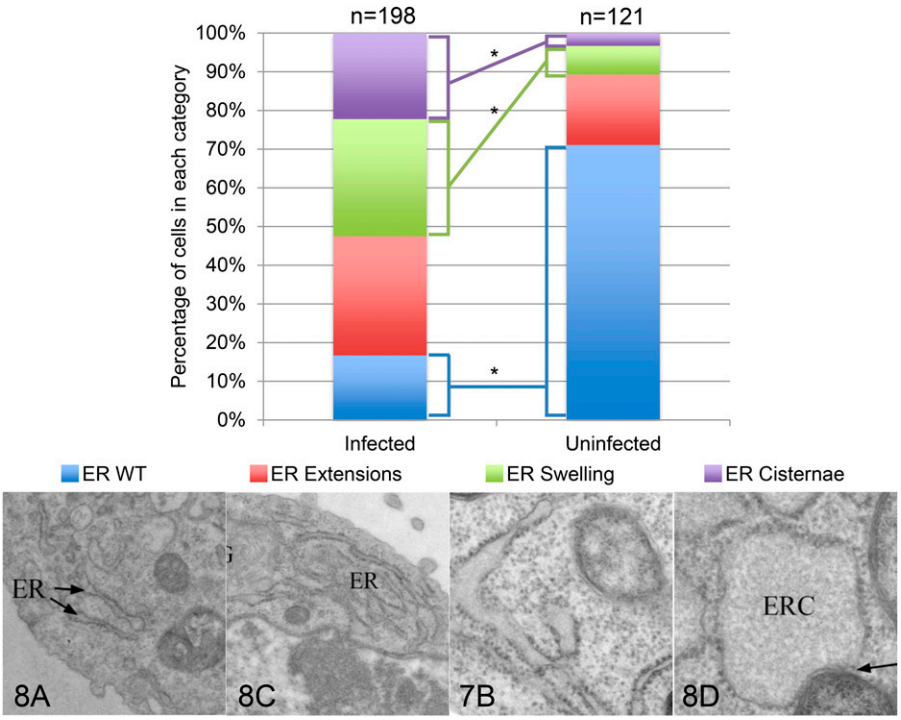

Figure 9 Quantification of ER morphology in *Wolbachia*-infected and cured cells. ER morphology in randomly selected EM sections from 198 *Wolbachia*-infected cells and 121 cured cells was classified into four distinct categories of ER morphology: wild type (WT), extensions, swelling, and cisternae. Quantification revealed the presence of *Wolbachia* significantly decreased the percentage of cells exhibiting wild-type ER and significantly increased the percentage of cells exhibiting ER swelling and ER cisternae ($P < 0.0001$ for all, with adjusted $\alpha = 0.00625$). Significance was determined using chi-square analysis. Images below illustrate each category. The number and letter in the bottom left of the images indicate which previous figure the image originated from. The ER and ER cisternae (ERC) are labeled where appropriate.

oocyte titer (Supplemental Material, Figure S1A). Three hits were also recovered in mitochondrial metabolism: a NADH dehydrogenase (CG3214), a succinate dehydrogenase (CG14757), and a mitochondrial carrier protein (CG18324). We found that knockdown of CG3214 and CG18324 in the *Drosophila* oocyte resulted in significant increases and decreases in *Wolbachia* titer, respectively (Figure S1, C and D). We suspect that the reduction of cellular ATP levels expected from knockdown of these genes limits the ability of *Wolbachia* to replicate within the cells. Alternatively, because specific *Wolbachia* and mitochondrial strains have coevolved, *Wolbachia* may be highly sensitive to functional changes in its companion mitochondria (Perlman *et al.* 2015). It should be pointed out that some of these RNAi hits might be false positives because secondary screens have not confirmed them.

Two hits that reduced *Wolbachia* titer were in genes regulating lipid metabolism. CG9243 encodes phospholipase D that catalyzes breakdown of phosphatidylcholine to phosphatidic acid and choline. CG1718 is an ABC transporter that functions in sterol uptake and esterification. This reliance on host lipid metabolism to maintain titer may be due to the fact that *Wolbachia* is encompassed by an outer host-derived membrane and lacks key fatty acid and cholesterol metabolic pathways (Voronin *et al.* 2004; Wu *et al.* 2004). Thus, replication of *Wolbachia* is likely to place exceptional demands on host lipid metabolism. Our results are also in accord with a recent study demonstrating that the presence of *Wolbachia* significantly alters lipid metabolism of *Aedes albopictus* mosquito cells (Molloy *et al.* 2016). Significantly, the titer of *Spiroplasma*, another maternally inherited insect endosymbiont, is also limited by the levels of host lipids (Herren *et al.* 2014). In addition, replication of mammalian pathogens *M. tuberculosis* and *C. trachomatis* requires host-derived lipids (Ehrt and Schnappinger 2007; Robertson *et al.* 2009).

It is now well documented that the presence of *Wolbachia* confers resistance against a number of positive-strand RNA viruses including dengue and Zika (Johnson 2015). There is evidence that multiple host mechanisms may be involved in inhibiting viral replication including synthesis of reactive oxygen and cholesterol and induction of host autophagy (Le Clec'h *et al.* 2012; Pan *et al.* 2012; Caragata *et al.* 2013; Wong *et al.* 2015). Our finding that *Wolbachia* dramatically alters host ER morphology and relies on the ERAD pathway to maintain titer suggests the involvement of a previously unsuspected mechanism in preventing the replication of positive-strand RNA viruses. For a number of positive-strand RNA viruses, the ER is the preferred site of replication and assembly (Romero-Brey and Bartenschlager 2016). Viral targeting of host ER induces dramatic changes in the morphology of the ER including invaginations of the ER membrane, swelling of the ER into large cisternae, and formation of virus-containing vesicles in the lumen (Romero-Brey and Bartenschlager 2016). These alterations are believed to create membrane-based sites of viral replication and assembly. Particularly striking are the recent findings that positive-strand RNA viruses specifically target and subvert the ERAD pathway to facilitate replication and assembly (Noack *et al.* 2014). For example, the ERAD pathway was identified in a recent genome-wide CRISPR (clustered regularly interspaced short palindromic repeats) screen to identify host factors essential to the dengue virus (Marceau *et al.* 2016). Our finding that *Wolbachia* also relies on the ERAD pathway for replication and produces dramatic alterations in ER morphology suggests that *Wolbachia* and positive-strand RNA viruses may be competing for the same intracellular niche. The intimate association between *Wolbachia* and the ER may physically prevent viruses from associating with ERAD sites. Alternatively, the extensive disruption in ER morphology may nonspecifically prevent the interactions necessary for viral replication. A satisfying aspect of this explanation of viral suppression is that it readily explains the ability of *Wolbachia* to suppress RNA viruses, and not DNA viruses, which preferentially replicate in the nucleus (den Boon *et al.* 2010). A number of other intracellular bacteria also exhibit a close association with the ER (Roy *et al.* 2006). It will be of great interest to determine whether these also suppress positive-strand RNA viral replication.

Acknowledgments

We thank the Sullivan laboratory members present and past for helpful discussion and suggestions as well as the Bloomington *Drosophila* Stock Center, the *Drosophila* community for reagents. We also thank Nadine Gassner, Frederic Landmann, Catharina Lindley, William C. Rice, and Gilles Hickson for assistance and advice. We thank Rémi Le Borgne from the ImagoSeine core facility of the Institut Jacques Monod, also associated with Infrastructure en Biologie Santé et Agronomie and France BioImaging infrastructures. Funding from National Institutes of Health grant GM-104486, University of California, Santa Cruz Faculty Research Award, and Florida International University supported this work. A.D. and A.G. were supported by the Centre National de la Recherche Scientifique, the Association de la Recherche sur le Cancer grant PJA 20141201756, and the "Ligue Contre le Cancer" grant RA11/75-34.

Author contributions: P.M.W., L.R.S., A.D., A.G., W.B., R.S.L., and W.S. designed the experiments. P.M.W., L.R.S., A.D., and A.C. conducted the experiments. P.M.W., L.R.S., A.D., and W.S. wrote the manuscript.

Literature Cited

Agaisse, H., L. S. Burrack, J. A. Philips, E. J. Rubin, N. Perrimon *et al.*, 2005 Genome-wide RNAi screen for host factors required for intracellular bacterial infection. Science 309: 1248–1251.

Agrawal, S., D. W. Chung, N. Ponts, G. G. van Dooren, J. Prudhomme *et al.*, 2013 An apicoplast localized ubiquitylation system is required for the import of nuclear-encoded plastid proteins. PLoS Pathog. 9: e1003426.

Akimana, C, S. Al-Khodor, and Y. Abu Kwaik, 2010 Host factors required for modulation of phagosome biogenesis and proliferation of Francisella tularensis within the cytosol. PLoS One 5: e11025.

Albertson, R., C. Casper-Lindley, J. Cao, U. Tram, and W. Sullivan, 2009 Symmetric and asymmetric mitotic segregation patterns

influence Wolbachia distribution in host somatic tissue. J. Cell Sci. 122: 4570–4583.
Ashton-Beaucage, D., C. Lemieux, C. M. Udell, M. Sahmi, S. Rochette *et al.*, 2016 The deubiquitinase USP47 stabilizes MAPK by counteracting the function of the N-end rule ligase POE/UBR4 in Drosophila. PLoS Biol. 14: e1002539.
Baldridge, G. D., A. S. Baldridge, B. A. Witthuhn, L. Higgins, T. W. Markowski *et al.*, 2014 Proteomic profiling of a robust Wolbachia infection in an Aedes albopictus mosquito cell line. Mol. Microbiol. 94: 537–556.
Beasley, T. M., and R. E. Schumacker, 1995 Multiple regression approach to analyzing contingency tables: post hoc and planned comparison procedures. J. Exp. Educ. 64(1): 79–93.
Brownlie, J. C., and S. L. O'Neill, 2005 Wolbachia genomes: insights into an intracellular lifestyle. Curr. Biol. 15: R507–R509.
Caragata, E. P., E. Rances, L. M. Hedges, A. W. Gofton, K. N. Johnson *et al.*, 2013 Dietary cholesterol modulates pathogen blocking by Wolbachia. PLoS Pathog. 9: e1003459.
Caragata, E. P., E. Rances, S. L. O'Neill, and E. A. McGraw, 2014 Competition for amino acids between Wolbachia and the mosquito host, Aedes aegypti. Microb. Ecol. 67: 205–218.
Chagas-Moutinho, V. A., R. Silva, W. de Souza, and M. C. Motta, 2015 Identification and ultrastructural characterization of the Wolbachia symbiont in Litomosoides chagasfilhoi. Parasit. Vectors 8: 74.
Debec, A., T. L. Megraw, and A. Guichet, 2016 Methods to establish Drosophila cell lines. Methods Mol. Biol. 1478: 333–351.
den Boon, J. A., A. Diaz, and P. Ahlquist, 2010 Cytoplasmic viral replication complexes. Cell Host Microbe 8: 77–85.
Derre, I., M. Pypaert, A. Dautry-Varsat, and H. Agaisse, 2007 RNAi screen in Drosophila cells reveals the involvement of the Tom complex in Chlamydia infection. PLoS Pathog. 3: 1446–1458.
Echard, A., G. R. Hickson, E. Foley, and P. H. O'Farrell, 2004 Terminal cytokinesis events uncovered after an RNAi screen. Curr. Biol. 14(18): 1685–1693.
Ehrt, S., and D. Schnappinger, 2007 Mycobacterium tuberculosis virulence: lipids inside and out. Nat. Med. 13: 284–285.
Everett, R. D., 2000 ICP0 induces the accumulation of colocalizing conjugated ubiquitin. J. Virol. 74: 9994–10005.
Fallon, A. M., and B. A. Witthuhn, 2009 Proteasome activity in a naive mosquito cell line infected with Wolbachia pipientis wAlbB. In Vitro Cell. Dev. Biol. Anim. 45: 460–466.
Ferree, P. M., H. M. Frydman, J. M. Li, J. Cao, E. Wieschaus *et al.*, 2005 Wolbachia utilizes host microtubules and dynein for anterior localization in the Drosophila oocyte. PLoS Pathog. 1: e14.
Foster, J., M. Ganatra, I. Kamal, J. Ware, K. Makarova *et al.*, 2005 The Wolbachia genome of Brugia malayi: endosymbiont evolution within a human pathogenic nematode. PLoS Biol. 3: e121.
Fujimuro, M., H. Sawada, and H. Yokosawa, 1994 Production and characterization of monoclonal antibodies specific to multi-ubiquitin chains of polyubiquitinated proteins. FEBS Lett. 349: 173–180.
Goshima, G., R. Wollman, S. S. Goodwin, N. Zhang, J. M. Scholey *et al.*, 2007 Genes required for mitotic spindle assembly in Drosophila S2 cells. Science 316: 417–421.
Herren, J. K., J. C. Paredes, F. Schupfer, K. Arafah, P. Bulet *et al.*, 2014 Insect endosymbiont proliferation is limited by lipid availability. eLife 3: e02964.
Hudson, A. M., and L. Cooley, 2014 Methods for studying oogenesis. Methods 68: 207–217.
Johnson, K. N., 2015 The impact of Wolbachia on virus infection in mosquitoes. Viruses 7: 5705–5717.
Karpova, N., Y. Bobinnec, S. Fouix, P. Huitorel, and A. Debec, 2006 Jupiter, a new Drosophila protein associated with microtubules. Cell Motil. Cytoskeleton 63: 301–312.
Kose, H., and T. L. Karr, 1995 Organization of Wolbachia pipientis in the Drosophila fertilized egg and embryo revealed by an anti-Wolbachia monoclonal antibody. Mech. Dev. 51: 275–288.
Le Clec'h, W., C. Braquart-Varnier, M. Raimond, J. B. Ferdy, D. Bouchon *et al.*, 2012 High virulence of Wolbachia after host switching: when autophagy hurts. PLoS Pathog. 8: e1002844.
Lemus, L., and V. Goder, 2014 Regulation of endoplasmic reticulum-associated protein degradation (ERAD) by ubiquitin. Cells 3: 824–847.
Marceau, C. D., A. S. Puschnik, K. Majzoub, Y. S. Ooi, S. M. Brewer *et al.*, 2016 Genetic dissection of Flaviviridae host factors through genome-scale CRISPR screens. Nature 535: 159–163.
Mazzalupo, S., and L. Cooley, 2006 Illuminating the role of caspases during Drosophila oogenesis. Cell Death Differ. 13(11): 1950–1959.
Metzger, M. B., M. J. Maurer, B. M. Dancy, and S. Michaelis, 2008 Degradation of a cytosolic protein requires endoplasmic reticulum-associated degradation machinery. J. Biol. Chem. 283: 32302–32316.
Min, K. T., and S. Benzer, 1997 Wolbachia, normally a symbiont of Drosophila, can be virulent, causing degeneration and early death. Proc. Natl. Acad. Sci. USA 94: 10792–10796.
Mohr, S. E., J. A. Smith, C. E. Shamu, R. A. Neumuller, and N. Perrimon, 2014 RNAi screening comes of age: improved techniques and complementary approaches. Nat. Rev. Mol. Cell Biol. 15: 591–600.
Molloy, J. C., U. Sommer, M. R. Viant, and S. P. Sinkins, 2016 Wolbachia modulates lipid metabolism in Aedes albopictus mosquito cells. Appl. Environ. Microbiol. 82: 3109–3120.
Moser, T. S., L. R. Sabin, and S. Cherry, 2010 RNAi screening for host factors involved in vaccinia virus infection using Drosophila cells. JoVE 42: e2137–e2137.
Mouton, L., H. Henri, M. Bouletreau, and F. Vavre, 2006 Effect of temperature on Wolbachia density and impact on cytoplasmic incompatibility. Parasitology 132: 49–56.
Muller, M. J., N. C. Dorr, M. Depra, H. J. Schmitz, V. H. Valiati *et al.*, 2013 Reevaluating the infection status by the Wolbachia endosymbiont in Drosophila Neotropical species from the willistoni subgroup. Infect. Genet. Evol. 19: 232–239.
Newton, I. L., O. Savytskyy, and K. B. Sheehan, 2015 Wolbachia utilize host actin for efficient maternal transmission in Drosophila melanogaster. PLoS Pathog. 11: e1004798.
Noack, J., R. Bernasconi, and M. Molinari, 2014 How viruses hijack the ERAD tuning machinery. J. Virol. 88: 10272–10275.
Pan, X., G. Zhou, J. Wu, G. Bian, P. Lu *et al.*, 2012 Wolbachia induces reactive oxygen species (ROS)-dependent activation of the Toll pathway to control dengue virus in the mosquito Aedes aegypti. Proc. Natl. Acad. Sci. USA 109: E23–E31.
Perlman, S. J., C. N. Hodson, P. T. Hamilton, G. P. Opit, and B. E. Gowen, 2015 Maternal transmission, sex ratio distortion, and mitochondria. Proc. Natl. Acad. Sci. USA 112: 10162–10168.
Philips, J. A., E. J. Rubin, and N. Perrimon, 2005 Drosophila RNAi screen reveals CD36 family member required for mycobacterial infection. Science 309: 1251–1253.
Pietri, J. E., H. DeBruhl, and W. Sullivan, 2016 The rich somatic life of Wolbachia. MicrobiologyOpen 5: 923–936.
Poinsot, D., K. Bourtzis, G. Markakis, C. Savakis, and H. Merçot, 1998 Wolbachia transfer from Drosophila melanogaster into D. simulans: host effect and cytoplasmic incompatibility relationships. Genetics 150(1): 227–237.
Robertson, D. K., L. Gu, R. K. Rowe, and W. L. Beatty, 2009 Inclusion biogenesis and reactivation of persistent Chlamydia trachomatis requires host cell sphingolipid biosynthesis. PLoS Pathog. 5: e1000664.
Romero-Brey, I., and R. Bartenschlager, 2016 Endoplasmic reticulum: the favorite intracellular niche for viral replication and assembly. Viruses 8: 160.
Roy, C. R., S. P. Salcedo, and J. P. Gorvel, 2006 Pathogen-endoplasmic-reticulum interactions: in through the out door. Nat. Rev. Immunol. 6: 136–147.
Serbus, L. R., and W. Sullivan, 2007 A cellular basis for Wolbachia recruitment to the host germline. PLoS Pathog. 3: e190.

Serbus, L. R., C. Casper-Lindley, F. Landmann, and W. Sullivan, 2008 The genetics and cell biology of Wolbachia-host interactions. Annu. Rev. Genet. 42: 683–707.

Serbus, L. R., A. Ferreccio, M. Zhukova, C. L. McMorris, E. Kiseleva *et al.*, 2011 A feedback loop between Wolbachia and the Drosophila gurken mRNP complex influences Wolbachia titer. J. Cell Sci. 124: 4299–4308.

Serbus, L. R., F. Landmann, W. M. Bray, P. M. White, J. Ruybal *et al.*, 2012 A cell-based screen reveals that the albendazole metabolite, albendazole sulfone, targets Wolbachia. PLoS Pathog. 8: e1002922.

Serbus, L. R., P. M. White, J. P. Silva, A. Rabe, L. Teixeira *et al.*, 2015 The impact of host diet on Wolbachia titer in Drosophila. PLoS Pathog. 11: e1004777.

Strunov, A., and E. Kiseleva, 2014 Drosophila melanogaster brain invasion: pathogenic Wolbachia in central nervous system of the fly. Insect Sci. 23: 253–264.

Unckless, R. L., L. M. Boelio, J. K. Herren, and J. Jaenike, 2009 Wolbachia as populations within individual insects: causes and consequences of density variation in natural populations. Proc. Biol. Sci. 276: 2805–2811.

Vaishnava, S., and B. Striepen, 2006 The cell biology of secondary endosymbiosis – how parasites build, divide and segregate the apicoplast. Mol. Microbiol. 61: 1380–1387.

Van Voorhis, W. C., J. H. Adams, R. Adelfio, V. Ahyong, M. H. Akabas *et al.*, 2016 Open source drug discovery with the malaria box compound collection for neglected diseases and beyond. PLoS Pathog. 12: e1005763.

Verheyen, E., and L. Cooley, 1994 Looking at oogenesis. Methods Cell Biol. 44: 545–561.

Voronin, D. A., N. V. Dudkina, and E. V. Kiseleva, 2004 A new form of symbiotic bacteria Wolbachia found in the endoplasmic reticulum of early embryos of Drosophila melanogaster. Dokl. Biol. Sci. 396: 227–229.

Werren, J. H., L. Baldo, and M. E. Clark, 2008 Wolbachia: master manipulators of invertebrate biology. Nat. Rev. Microbiol. 6: 741–751.

Wong, Z. S., J. C. Brownlie, and K. N. Johnson, 2015 Oxidative stress correlates with Wolbachia-mediated antiviral protection in Wolbachia-Drosophila associations. Appl. Environ. Microbiol. 81: 3001–3005.

Wu, M., L. V. Sun, J. Vamathevan, M. Riegler, R. Deboy *et al.*, 2004 Phylogenomics of the reproductive parasite Wolbachia pipientis wMel: a streamlined genome overrun by mobile genetic elements. PLoS Biol. 2: E69.

Yang, H., K. R. Landis-Piwowar, D. Chen, V. Milacic, and Q. P. Dou, 2008 Natural compounds with proteasome inhibitory activity for cancer prevention and treatment. Curr. Protein Pept. Sci. 9: 227–239.

Zhang, J. H., T. D. Chung, and K. R. Oldenburg, 1999 A simple statistical parameter for use in evaluation and validation of high throughput screening assays. J. Biomol. Screen. 4(2): 67–73.

Zhou, Y., and Y. Zhu, 2015 Diversity of bacterial manipulation of the host ubiquitin pathways. Cell. Microbiol. 17: 26–34.

Communicating editor: D. A. Barbash